2013

A unified perspective on traffic flow theory. Part III: Validation and benchmarking

Daiheng Ni, *University of Massachusetts - Amherst*
Haizhong Wang

Applied Mathematical Sciences, Vol. 7, 2013, no. 40, 1965 - 1982
HIKARI Ltd, www.m-hikari.com

A Unified Perspective on Traffic Flow Theory Part III: Validation and Benchmarking

Daiheng Ni

Department of Civil and Environmental Engineering
University of Massachusetts, Amherst, MA 01003, USA
ni@ecs.umass.edu

Haizhong Wang

School of Civil and Construction Engineering
Oregon State University, Corvallis, OR 97331, USA

Abstract

A Field Theory of traffic flow was formulated, based on which a special case, called Longitudinal Control Model, was proposed in Part I. The objective of this paper is to evaluate the model. A set of reasonable criteria was employed in the assessment including: empirical validity, mathematical elegance, and physical soundness. Both numerical and empirical evidences are presented in support of the model. In addition, a cross-comparison, called benchmarking, was conducted to show the performance of the model relative to some existing traffic flow models.

Keywords: Mathematical modeling, field theory, traffic flow theory

1 INTRODUCTION

Over more than half a century, traffic flow theorists have been pursuing two goals: (i) simple and efficient models to abstract vehicular traffic flow and (ii) a unified framework in which existing traffic flow models fit and relate to each other. In response to the second goal, a framework and consequently a Unified

Diagram has been presented in Part II. In that paper traffic flow models at both microscopic and macroscopic levels are directly or indirectly related to the Field Theory that is formulated in Part I.

The first goal gives rise to the issue of how to evaluate models. Unfortunately, a set of commonly agreed evaluation criteria has yet to be devised since this is a subjective matter. Nevertheless, the following proposition may be approved by many: *empirical* validity, *mathematical* elegance, and *physical* soundness, which are further elaborated as follows.

Empirical Validity

A model is empirically valid if it agrees well with observations in the laboratory and the field.

Mathematical Elegance

A model is mathematically elegant if it summarizes the underlying process using the least number of equations (ideally one equation for all) in simple functional form involving the least number of parameters/coefficients. Take car-following models for example, General Motors (GM) models (1; 2) involve one equation, Gipps (3) model consists of two equations, psycho-physical models (4) features multiple equations, rule-based models (5; 6) utilizes a set of fuzzy decision rules rather than mathematical equations, and agent-based models (7) employ artificial intelligence (e.g. neural networks) to make decisions. As one moves along this list, the models become increasingly intelligent. Meanwhile, their mathematical tractability progressively diminishes.

Physical Soundness

A model is physically sound if it is able to capture the underlying mechanism of the target system in a way that is consistent with first principles (such as Newton's laws of motion or Maxwell's equations of electromagnetism). In general, there are two modeling approaches: *descriptive* vs. *explanatory*. The descriptive approach focuses on fitting the model to observed behavior of the target system without worrying about how the system works, while the explanatory approach looks behind the scene and tries to represent the underlying principle by following its chain of reasoning. For example, Greenshields (8) model stipulates that when traffic density is x traffic speed ought to be y, but the model could not explain why this is the case. In contrast, Gipps (3) model predicts that a driver moving at v km per hour is likely to leave a spacing of s m ahead. This is so because it is calculated from the driver's control strategy which guarantees his or her safety in case that the leader applies emergency

brake. Though descriptive models may be simpler in some cases, explanatory models are generally more informative and traceable.

In addition, it is desirable that a microscopic model aggregates to known macroscopic behavior and a macroscopic model has a sound microscopic basis. For example, a car-following model describes the behavior of individual vehicles. Aggregation of such behavior over vehicles and time gives rise to a macroscopic speed-density relationship. Hence, a sound car-following model would statistically agree with observed relation between traffic speed and density. Conversely, a sound macroscopic speed-density model should be rooted in or can be derived from a valid car-following model. Such a micro-macro coupling is attractive because it allows an additional, complementary perspective on the same system and thus it may be more efficient to identify and address operational deficiencies of the system.

Moreover, it is preferable that a model employs parameters that are physically meaningful and easy to calibrate. Model parameters can be roughly divided into the following three categories: (1) Parameters with physical meaning and easy to calibrate. For example, the calibration involves only small-scale data collection, based on which it is relatively easy to determine the values of the parameters. Included in this category are desired speed, perception-reaction time, vehicle length, maximum acceleration, free-flow speed, jam density, capacity, etc. (2) Parameters with physical meaning but difficult to calibrate. For example, the calibration involves large-scale data collection, from which it is complicated to determine parameter values. Included in this category are critical density, optimal speed, breakdown flow, etc. (3) Coefficients that need calibration and without physical meaning.

With the above understanding, the objective of this paper is to evaluate the Longitudinal Control Model (LCM) proposed in Part I. It is easy to verify that LCM is physically sound for the following reasons: it is derived from the Field Theory which has its roots in classical physics and social science; it is formulated by taking an explanatory approach to capture the underlying principles of motion; there is a tight coupling between microscopic and macroscopic versions of LCM; LCM employs only category 1 parameters. In addition, it is evident that LCM is mathematically elegant since it is a one-equation model that applies to all operating conditions. Therefore, the rest of the paper will focus on empirical validity of LCM. First, the validity of LCM will be assessed by comparing against empirical observations and the comparison will be conducted at both microscopic and macroscopic levels (Section 2). In addition, it is interesting to cross-compare LCM with some of the well-established models presented in the Unified Diagram. This will be accomplished by benchmarking these models against a common set of data (Section 3). Finally, concluding remarks will be presented in Section 4.

2 VALIDATION

In Part I, the microscopic version of LCM was proposed based on Field Theory and the macroscopic version of LCM was derived from its microscopic counterpart. For easy reference, major equations of LCM are summarized below.

Longitudinal Control Model (microscopic):

$$\ddot{x}_i(t+\tau_i) = g_i[1 - (\frac{\dot{x}_i(t)}{v_i}) - e^{\frac{s_{ij}(t)^* - s_{ij}(t)}{s_{ij}(t)^*}}] \tag{1}$$

$$s^*_{ij}(t) = \frac{\dot{x}^2_i(t)}{2b_i} + \dot{x}_i(t)\tau_i - \frac{\dot{x}^2_j(t)}{2B_j} + l_j \tag{2}$$

Longitudinal Control Model (macroscopic):

$$v = v_f[1 - e^{1 - \frac{1}{k(v\tau' + l)}}] \tag{3}$$

$$k = \frac{1}{(v\tau' + l)[1 - ln(1 - \frac{v}{v_f})]} \tag{4}$$

2.1 Microscopic Validation

Validation at the microscopic level focuses on comparing model output against observations of individual driver-vehicle behavior. The comparison is conducted on acceleration, deceleration, and car-following performances.

2.1.1 Acceleration Performance

Figure 1 shows the acceleration performance of the Longitudinal Control Model which accelerates a vehicle from stand-still to a pre-determined desired speed without being impeded by other vehicles. The simulation is set up as follows: $g_i = 4$ m/s^2, $v_i = 40$ m/s, $\tau_i = 1$ s, $b_i = 4$ m/s^2, $B_j = 6$ m/s^2, and $s_{ij} = \infty$. The top-left figure is displacement-time plot, the top-right speed-time curve, bottom-left acceleration-time plot, and the bottom-right tabulates part of the simulation data (left 4 columns).

According to Motor Trend road tests, it takes about 10.4 seconds to accelerate a passenger car from 0 to 26.8 m/s (60 mph) and 17.8 seconds to traverse a quarter mile (about 402 m). The Longitudinal Control Model predicts that 0-60 mph time is about 10.5 seconds and quarter mile time is 17.7 seconds. The two sets of results agree well. In addition, the model performance is close to NCHRP speed on acceleration (9) in the last two columns of the table.

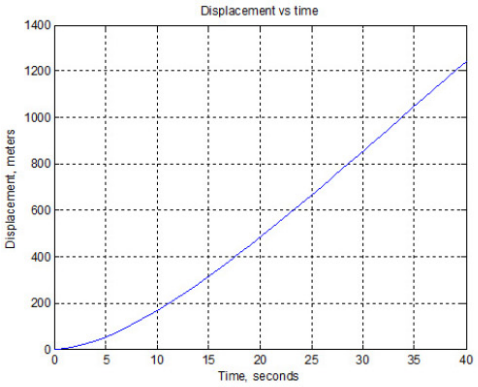

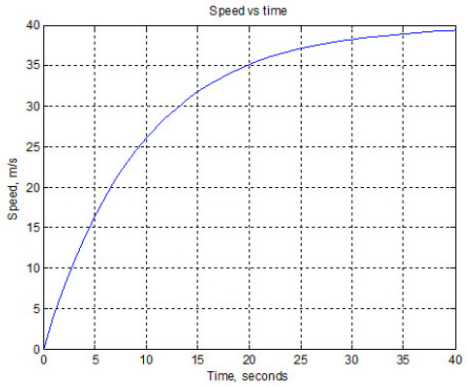

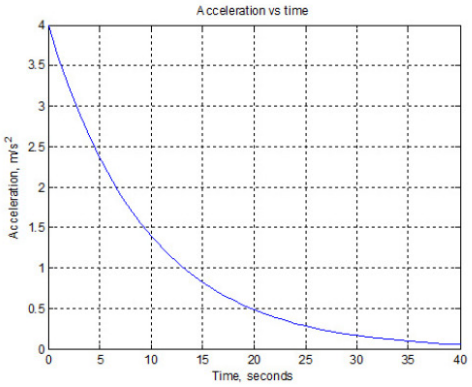

Time (s)	x (m)	v (m/s)	a (m/s^2)	v' (m/s)	a' (m/s^2)
2	11.6	7.6	3.2		
4	36.2	13.8	2.6	13.4	2.7
6	71.3	18.7	2.1	17.9	2.2
8	115.0	22.8	1.7	22.4	1.8
10	165.5	26.0	1.4	26.8	1.6
11	193.0	27.4	1.3		
15	314.1	31.8	0.8		
18	413.9	34.0	0.6		
20	483.6	35.1	0.5		
25	665.5	37.1	0.3		
30	854.6	38.2	0.2		
35	1048.0	38.9	0.1		
40	1243.9	39.3	0.1		

Figure 1: Acceleration performance

2.1.2 Deceleration Performance

Figure 2 shows the deceleration performance of the Longitudinal Control Model which brings a vehicle to a stop behind a stationary object (a stop line or a stopped vehicle). The simulation is set up as follows: initial speed $\dot{x}_i = 48$ m/s, initial position $x_i = -1127$ m, $x_j = 0$ m constantly, $g_i = 4$ m/s^2, $v_i = 50$ m/s, $\tau_i = 1$ s, $b_i = 4$ m/s^2, $B_j = 6$ m/s^2. The top-left figure is displacement-time plot, the top-right speed-time curve, bottom-left acceleration-time plot, and the bottom-right tabulates part of the simulation data (left three columns). The model performance is compared against Part 571 of the Federal Motor Vehicle Safety Standards - Standard No. 105 (10) published by the Federal Motor Carrier Safety Administration (FMCSA). The purpose of the standard is to ensure safe braking performance under normal and emergency conditions. The FMCSA standard, which is listed in the last two columns of the table, stipulates the distances required to decelerate a vehicle to a stop from its initial speeds. For example, a passenger car should be able to come to rest from 26.8 m/s (60 mph) within 65.8 m (216 ft). A comparison of the numbers suggests that the acceleration performance of the Longitudinal Control Model agrees reasonably with those in the FMCSA standard.

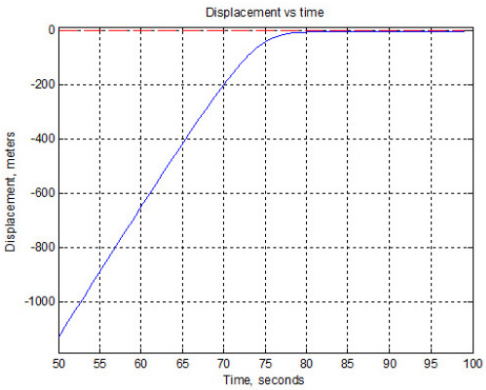

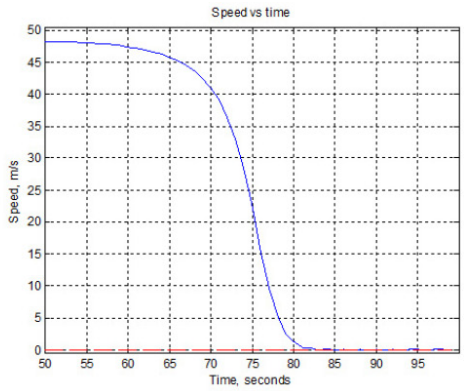

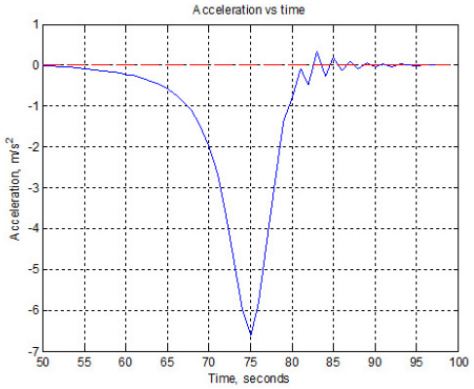

x (m)	v (m/s)	a (m/s^2)	v' (m/s)	x' (m)
364.7	45.2	-0.7		
320.2	44.5	-0.9	44.7	205.1
276.6	43.6	-1.2		
234.2	42.4	-1.5		
193.2	40.9	-2.0		
154.2	39.0	-2.6		
117.9	36.3	-3.6	35.8	123.4
85.1	32.8	-4.7		
57.1	28.0	-6.0	26.8	65.8
35.1	22.0	-6.6		
19.6	15.4	-5.8	13.4	16.5
10.0	9.6	-4.3		
0.0	0.0	0.0		

Figure 2: Deceleration performance

2.1.3 Car-Following Performance

Three sets of trajectory data are used: NGSIM (11), JHK (12), and IVBSS (13). Pairs of vehicles in car following are identified. For each pair, the leading vehicle's trajectory, speed, and acceleration are used as input, against which the model simulates the follower. Then the performances of the leading vehicle (observed) and the following vehicle (both observed and simulated) are plotted on the same figure for comparison. The objective is to investigate whether the model, after being tuned over a reasonable range, is capable of reproducing the observed car-following behavior.

Figure 3 shows the results of car-following pair 1388-1386 (leader-follower). The top-left figure is displacement-time plot, the top-right speed-time plot, and bottom-left acceleration-time plot. The leader (observed) is illustrated using solid black lines, the follower (observed) dash blue lines, and the follower (simulated) dotted red lines. The bottom-right shows errors/residues of displacement (solid black line, m), speed (dash blue line, m/s), and acceleration (dotted red line, m/s^2)-time. As discussed before, the key issue here is to examine the model's ability to reproduce the follower's behavior. In addition to assessing the quality of approximation, one needs to verify if the simulated

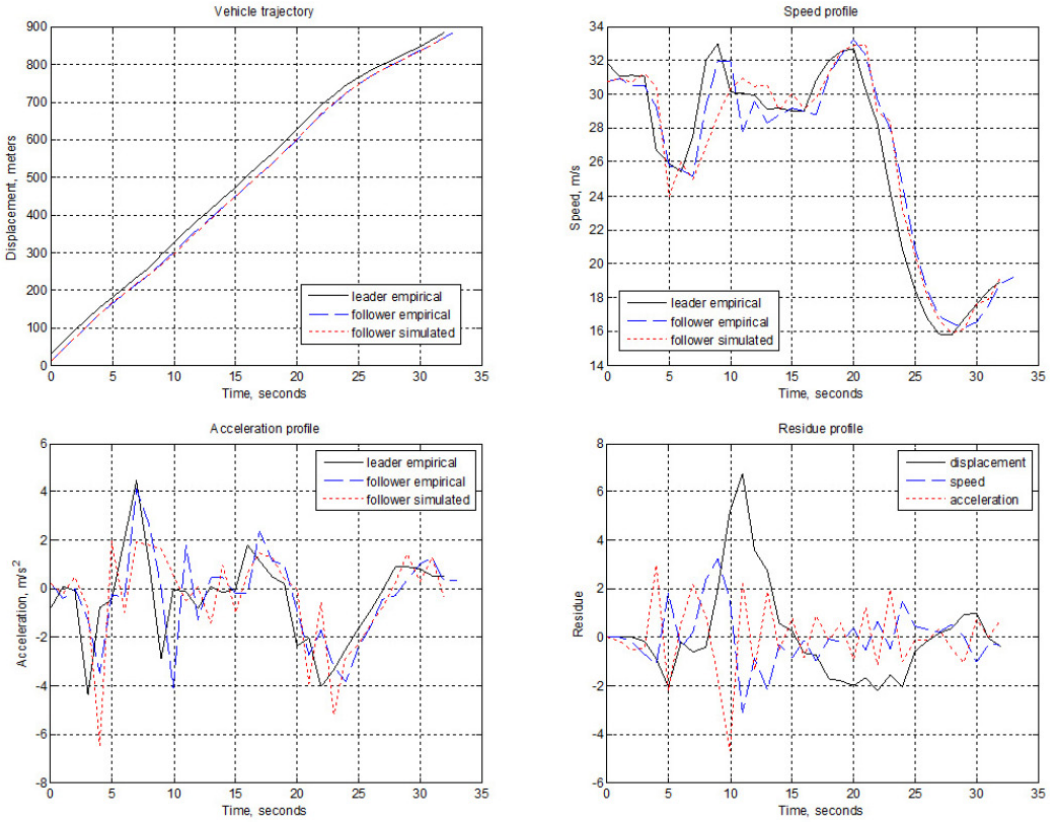

Figure 3: Car following performance

follower exhibits unacceptable behaviors such as crossing over its leader (which signifies a crash), moving backwards (which involves negative speeds), being out of pace with the empirical follower, particularly in the speed profile (which breaks car following), etc. Model parameters and comparison results of all car-following pairs are presented below.

In Figure 4, the first column identifies data source (e.g., NGSIM) and car-following pair (e.g., 1388-1386). The third columns shows the mean ("Mean") and standard deviation ("STD") of simulation error of displacement. The fourth and fifth columns displaces "Mean" and "STD" of simulation error of speed and acceleration, respectively.

Figure 5 lists values of parameters of LCM used to run the simulation.

2.2 Macroscopic Validation

The data used in this validation are collected at multiple locations including: Georgia 400 in Atlanta, Autobahn in Germany, I-4 in Florida, Highway 401 in Canada, Amsterdam Ring Road, and I-80 in California. For each set of data,

		x (m)	v (m/s)	a (m/s^2)
NGSIM	Mean	-0.04	-0.01	0.06
1388-1386	STD	2.26	1.19	1.32
NGSIM	Mean	-0.04	-0.01	0.06
3011-3012	STD	2.57	1.15	1.23
NGSIM	Mean	0.04	-0.20	-0.02
4022-2193	STD	4.49	1.22	1.25
JHK	Mean	0.00	-0.09	0.01
935-936	STD	1.00	1.44	2.51
JHK	Mean	-0.02	-0.02	-0.06
2666-2668	STD	0.98	1.28	2.26
JHK	Mean	0.06	0.25	0.04
4042-4045	STD	3.15	1.17	1.80
IVBSS	Mean	1.42	-0.02	-0.01
	STD	8.64	1.19	1.03

Figure 4: Car following validation results

	τ_i (s)	V_i (m/s)	L_j (m)	g_i (m/s^2)	b_i (m/s^2)	B_j (m/s^2)
1388-1386	0.3	40	4.3	6	6	6
3011-3012	0.4	40	4.3	6	6	6
4022-2193	0.6	41	4.3	6	6	6
935-936	0.5	34	4.6	6	6	6
2666-2668	0.7	32	4.6	6	6	6
4042-4045	1.5	28	4.6	6	6	6
IVBSS	0.4	36	5	6	6	6

Figure 5: Car following validation parameters

the comparison of empirical observations and model performance are presented in their underlying fundamental diagrams (a fundamental diagram is a set of graphics including speed-density, speed-flow, flow-density, and speed-spacing plots). Figure 6 presents the observed and simulated fundamental diagrams based on GA4001116 data. The top-left part is speed-density plot, the top-right speed-flow plot, the bottom-left flow-density plot, and the bottom-right speed-spacing plot. In each plot, empirical observations ("Empirical") are scattered as small dots ("the cloud") and the simulated data ("LCM") are shown as solid lines. In addition, empirical observations are averaged with respect to density and the results ("Emp mean") are displayed as large dots. With the four plots of the fundamental diagram, the figure provides the full perspective needed to assess the overall performance of a macroscopic equilibrium model from complementary angles. In each data set, the speed-density and speed-spacing plots appear to show encouraging results, while the flow-density and speed-flow plots (particularly the latter) tend to reveal problems. In the speed-flow plot, the empirical data seem to suggest an almost flat upper branch, i.e. the shape has a pointy "nose" that skews upward, which gives rise to a high optimal speed and a low optimal density at capacity. However, the model only exhibits a round nose, though it does lean upward in some cases. In addition, the model extrapolates a jam density of about 250 veh/km in some cases which

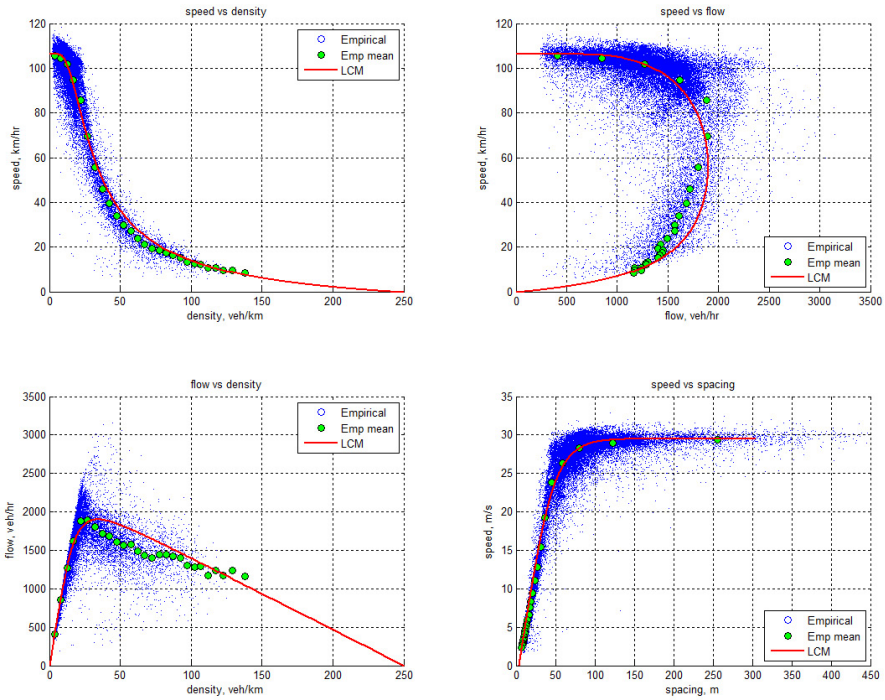

Figure 6: Comparison of fundamental diagrams (GA4001116 data)

translates to about an average inter-vehicle spacing of 4 m which is quite small unless the vehicles are predominantly compact cars with regular commuters (This observation was prompted by Dr. Martin Treiber's work). Except for these, the model in general agrees well with the empirical data, especially in good match with the aggregated observations ("Emp mean").

			LCM			Empirical		
Data set	v_f (km/hr)	k_j (v/km)	q_m (v/hr)	v_m (km/hr)	k_m (v/km)	q_m (v/hr)	v_m (km/hr)	k_m (v/km)
GA4001116	106.2	250.0	1900.0	56.0	33.9	1887.0	69.4	27.2
GA4001120	104.4	250.0	2123.0	56.6	37.5	2145.0	78.5	27.3
GA4001139	104.4	200.0	1990.0	58.0	34.3	1978.0	72.2	27.4
Autobahn	155.9	83.3	2085.6	95.4	21.9	2114.0	95.0	22.3
I-4	88.2	83.3	1825.0	58.0	31.5	1785.0	70.0	25.5
Hwy401	106.2	83.3	1870.6	68.0	27.5	1946.0	89.1	21.8
Amsterdam	102.2	90.9	2509.0	68.0	36.9	2452.0	90.3	27.2
I-80	111.6	158.7	1181.0	58.3	20.3	1125.0	102.5	11.0

Figure 7: Macroscopic validation numerical results

Comparison with empirical data from other sites exhibits similar pattern and the result is summarized in Figure 7. The fist column identifies data sources (e.g., GA4001116). The second and third columns are parameters of

LCM fitted to the data. Columns four to six show capacity condition (i.e., capacity q_m and associated optimal speed v_m and density k_m) predicted by LCM model, while columns seven to nine list capacity condition observed in the data. It can be seen that the model predicts capacity very well, but predicts optimal speed and density with varying success. In general, optimal densities match closer that optimal speed. As discussed above, the lack of fit in optimal speed and density is due to the "round nose" exhibited by the LCM and the reason is because LCM employs only three parameters which provides only limited flexibility in fitting the data. Nevertheless, compared with other three-parameter models, the performance of LCM is satisfactory, see Figure 10.

3 BENCHMARKING

At this point, the Field Theory and its special case, the Longitudinal Control Model, have been formulated and supporting evidences presented. Next, it would be interesting to cross-compare this model with other well-established traffic flow models. The goal is to provide a glimpse of the diversity of modeling flavors and how they complement each other and contribute to traffic flow theory. To accomplish this goal, a common ground is set up, on which each of the candidate models demonstrates so that their performances can be related to each other by referencing to the common ground. Such a process is called benchmarking and the common ground consists of a set of data at both microscopic and macroscopic levels and of numerical and empirical nature.

3.1 Microscopic Benchmarking

3.1.1 Model Selection

A subset of the microscopic car-following models presented in the Unified Diagram were selected including: General Motors 4th generation model (GM4) (1; 2), Gipps car-following model (3), Intelligent Driver Model (IDM) (14; 15), Newell non-linear car-following model (16), and Van Aerde car-following model (17; 18). The selection mainly considers those with analytical forms to facilitate implementation and comparison.

3.1.2 Benchmarking Scenario

Though the vehicle trajectory data sets used in the above microscopic validation can serve the purpose of microscopic benchmarking, they include only limited regimes that a driver might encounter in a real system, i.e. these data sets depict primarily the car-following regime with very few to no samples in

other regimes such as free flow, approaching, stopping, and cutting off. To incorporate these regimes in a single driving process yet without loosing credibility, a hypothetical scenario that makes physical sense is devised as follows. The scenario involves two vehicles: a leading vehicle j and a following vehicle i. The motion of the leader is pre-determined and that of the follower is governed by a car-following model under consideration. Initially (at $t = 0$), vehicle j parks at 5000 meters downstream from the origin ($x_j(0) = 5000$ m, $\dot{x}_j(0) = 0$ m/s, and $\ddot{x}_j(0) = 0$ m/s^2). Vehicle i, which is also still ($\dot{x}_i(0) = 0$ m/s and $\ddot{x}_i(0) = 0$ m/s^2), waits somewhere upstream of the origin and the distance is to be determined. When the scenario starts ($t > 0$), vehicle j remains parked but vehicle i starts to move according to a selected model. Since vehicle j is far ahead, vehicle i is entitled to accelerate freely to satisfy its desire for mobility. At time $t = 100$ s, vehicle i is at about 2770 m downstream of the origin (with this distance one can back calculate where the vehicle needs to start initially according to the model). At this moment, a third vehicle previously moving in the adjacent lane at 24 m/s changes to the subject lane at location 2810 m and takes over as the new leading vehicle j (the parked vehicle is now removed from the road), i.e. $x_j(100) = 2810$ m, $\dot{x}_j(100) = 24$ m/s, and $\ddot{x}_j(100) = 0$ m/s^2. This change is designed to mimic the cutting-off effect. The new leading vehicle keeps moving at the speed till $t = 200$ s, and then undergoes a deceleration process at a rate of $\ddot{x}_j = -3$ m/s^2 till it comes to a complete stop. After that, vehicle j remains stopped till $t = 300$ s. Then, it begins to accelerate at a constant rate of $\ddot{x}_j = 2$ m/s^2 and eventually settles at its full speed of $\dot{x}_j = 36$ m/s. At time $t = 400$ s. The vehicle starts to decelerate again at a constant rate of $\ddot{x}_j = -3$ m/s^2 till it comes to another full stop and remains there till the end. During all the time, the motion of the follower i is completely stipulated by the selected model.

This scenario includes a series of tests in a single driving process. Rather than seeking "the best" model, our focus here is to analyze whether a model makes physical sense when facing these tests. Therefore, items to be checked in the benchmarking are:

- Start-up: whether the model itself is sufficient to start the vehicle up or additional, external logic is needed.
- Speed-up: whether the model generates speed and acceleration profiles that make physical sense.
- Free flow: whether the model settles at its desired speed without oscillation.
- Cutting-off: whether the model loses control or, if not, responds with reasonable control maneuver.
- Following: whether the model is able to adopt the leader's speed and follow the leader within reasonable distance.

- Stop-and-go: whether the model is able to stop the vehicle safely behind its leader and start moving when the leader departs.
- Trailing: whether the model is able to speed up normally without being tempted by its speeding leader.
- Approaching: whether the model is able to adjust the vehicle properly when the gap closes up.
- Stopping: whether the model is able to stop the vehicle properly behind a stationary object, e.g. with oscillation, separated by a minimum spacing, speed and acceleration dropping to zero when stopped, etc.

The starting position of the follower i is determined by trial-and-error such that the vehicle moves to $x_i \approx 2770$ m at $t = 100$ s, at which point the vehicle should have reached its desired speed $v_i = 30$ m/s. The sudden appearance of the new leader j at $x_j = 2810$ m leaves a spacing of about 40 m between the two vehicles, which is a little more than the distance traversed during perception-reaction time. Drivers would normally back up and then seek a comfortable distance to start car following.

3.1.3 Benchmarking Results

Benchmarking results are plotted along with the performance of the leading vehicle and the Longitudinal Control Model in Figure 8. From top to bottom, the figure shows displacement-time, speed-time, and acceleration-time plots, respectively. In each plot, the performance of the leader j is pre-determined and depicted as the black solid line and the performance of the follower i simulated by models are plotted as dashed or dotted lines.

Values of model parameters used in this microscopic benchmarking is listed in Figure 9. When determining values of model parameters, those suggested in the original papers are adopted by default. However, if a default value leads to inferior performance, an appropriate replacement will be sought with good faith.

These models can be divided into two groups: dynamic models (LCM, GM4, and IDM) and steady-state models (Gipps, Newell, and Van Aerde). A known issue with steady-state models is the extreme acceleration at start-up, i.e. the model allows a vehicle's speed to increase from zero to an arbitrary high speed (e.g. 30 m/s) resulting an unrealistic acceleration (e.g. 30 m/s^2). Hence, an external logic has to be applied to constrain the maximum acceleration. In addition, a another external logic is needed to constrain the performance of acceleration on speed, i.e. as speed increases, acceleration decreases till it vanishes at the achievement of desired speed. Gipps model is an exception since it trades model elegance (i.e. its two-piece formulation) for realistic acceleration performance. Overall, these models perform very well except for the known

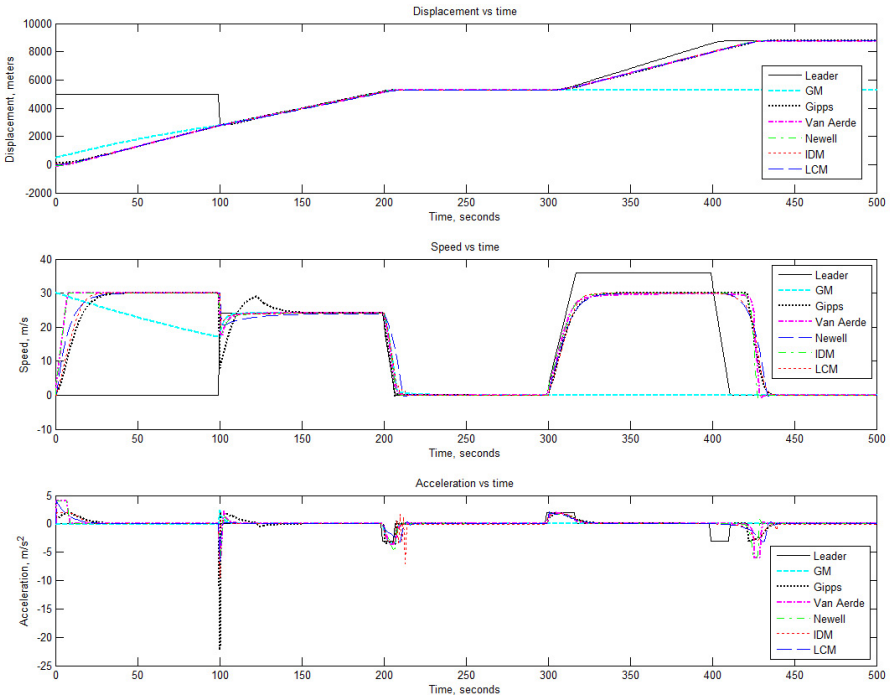

Figure 8: Microscopic benchmarking

issues of GM model (nevertheless, it necessitates only two parameters), especially considering the series of challenging tests faced by models with such simple and elegant forms.

3.2 Macroscopic Benchmarking

3.2.1 Model Selection

A subset of the macroscopic equilibrium models presented in the Unified Diagram were selected including: Newell model (16), Del Castillo model (19; 20), Intelligent Driver Model (IDM) (14; 15), and Van Aerde model (17; 18). The considerations of model choice include (1) single-regime models with analytical form, (2) models with sound microscopic basis, preferably those derived from their microscopic counterparts, and (3) models with known satisfactory performance.

Model	τ_i (s)	v_i (m/s)	L_j (m)	g_i (m/s^2)	b_i (m/s^2)	*More*	
LCM	1	30	5	4	4	$B_j = 6$ m/s^2	
GM4	1	-	-	-	-	$\alpha = 0.8$	
Gipps	1.1	30	6.5	1.7	3.4	$B_j = 3.2$ m/s^2	
IDM	T=1.6	30	5	0.73	1.67	$\delta = 4$	$s_0 = 2$
Newell	1	30	5	-	-	$\lambda = 0.79$ 1/s	
Van Ader	1	30			$v_c = 25$ m/s	$q_c = 2/3$ v/s	$k_j = 143$ v/km

Figure 9: Microscopic benchmarking parameters

3.2.2 Benchmarking Scenario

The data set collected at GA4001116 is used for macroscopic Benchmarking. Since other data sets used in the macroscopic validation provide similar information, their results are not repeated here.

3.2.3 Benchmarking Results

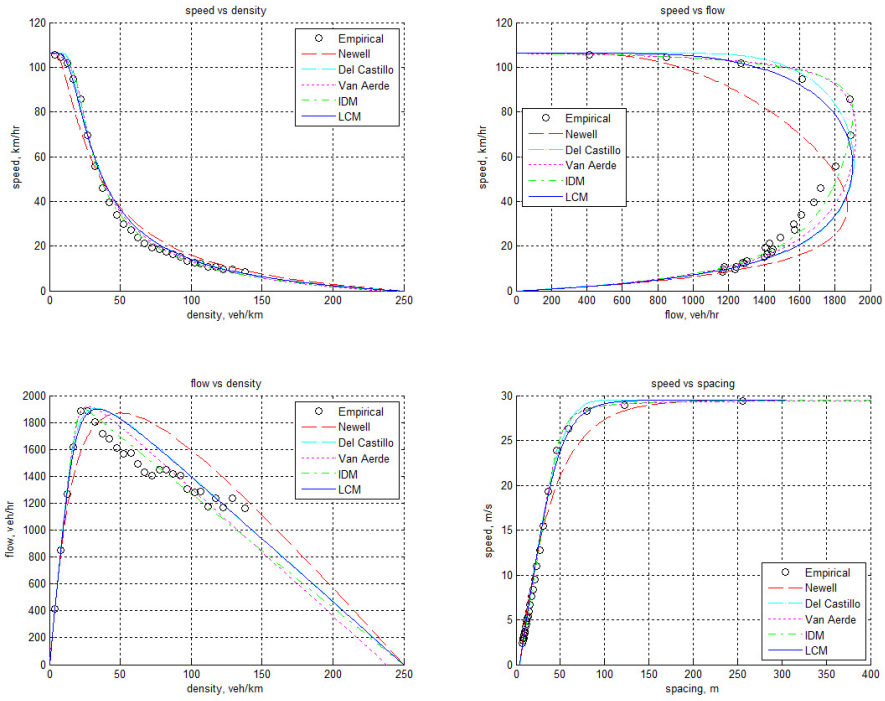

Figure 10: Macroscopic benchmarking: GA4001116

When fitting models to the data, free-flow speed is first determined since this information is readily available in the data. Then jam density is determined by following the trend of the congested portion of the flow-density plot.

With these two parameters set, other parameters are fine-tuned to achieve satisfactory results. Though each model is fitted to the data with good faith, there is no guarantee that the fitting results are optimal. Nevertheless, the results are able to reveal some critical properties of these models. Fitted models are plotted in Figure 10 along with empirical data (aggregated with respect to density). Additional information regarding model parameters and benchmarking results are presented in Figures 11 and 12.

Model	v_f (km/h)	k_j (v/km)	More	
Newell	106.2	250	λ=0.79 1/s	
Del Castillo	106.2	250	$\|C_j\|$ = 2.6 m/s	
Van Ader	106.2	250	v_c = 72 km/r	q_c = 1950 v/h
IDM	106.2	250	t=1.7 s	δ = 15
LCM	106.2	250	τ=1.4 s	

Figure 11: Macroscopic benchmarking parameters (Data: GA4001116)

Overall, these models demonstrates very satisfactory performance, especially considering their simple elegant forms, a variety of regimes over the full density range, and the quality of fitting. For example, all of them have clearly defined free-flow speed v_f and jam density k_j which agree with the data well. All of the flow-density curves exhibit a concave shape and match the capacity q_m well. Their discrepancies, in a picky eye, are mainly related to the capacity condition (i.e. k_m and v_m when capacity occurs). In the speed-flow plot, the capacity is illustrated as the "nose" of each curve. Newell model has its nose pointing downward which is less than ideal, the noses of Del Castillo model and LCM point forward which is quite close (Del Castillo model appears even closer than LCM), and the noses of Van Aerde model and IDM lean upward which is desirable, see figures in Subsection 2.2 (those with the "cloud") for a confirmation of such a shape). These discrepancies give rise to the effects that the "peaks" of the flow-density curves are skewed toward the left in varying degrees, and that the "corners" of the speed-spacing curves are sharpened to varying extent. However, on a positive note, Newell model, Del Castillo model, and LCM are satisfactory since they necessitate only three parameters with Newell model featuring a particularly simple, closed form of $v(k)$. It is interesting to note that a four-parameter LCM is under investigation and our preliminary result shows that this model is flexible enough to fit typical shapes of flow-density plot such as a skewed parabola, a triangular shape, and even an inverse-lambda shape.

Model	v_f	k_j	v_m	k_m	q_m	λ	q-k shape
Newell	√	√	low	high	√	close	concave
Del Castillo	√	√	close	close	√	√	concave
Van Ader	√	√	√	√	√	√	concave
IDM	√	√	√	√	√	√	concave
LCM	√	√	close	close	√	√	concave

√ denotes satisfactory performance

Figure 12: Macroscopic benchmarking results (Data: GA4001116)

4 CONCLUSION

The focus of this paper is to validate LCM and cross-compare with a set of well-established traffic flow models. The microscopic validation compares the model's acceleration, deceleration, and car-follow performances against road test results, established standard, and empirical observations. Comparison results suggested that the model is able to realistically accelerate and decelerate a vehicle in a manner that complies with road test results and regulation standard. When a leading vehicle is present, the model was able to reproduce car-following behavior with reasonable accuracy. The macroscopic validation compares the model's macroscopic performance against observed speed-density, speed-flow, flow-density, and speed-spacing relationships. In general, the model agrees well with the empirical data except that the predicted optimal speed is lower than observed.

A benchmarking was conducted in which LCM and other models are compared against the same sets of data. The microscopic benchmarking uses a hypothetical scenario where multiple regimes are integrated into one driving process. All the microscopic models performed well except for the known issues of the GM model and the acceleration issue with steady-state models. The macroscopic benchmarking was based on comparing observed and predicted fundamental diagrams. All the macroscopic equilibrium models are able to fit empirical data with reasonable accuracy except for some discrepancies under capacity conditions. More specifically, Van Aerde model and IDM fit the data best, and Del Castillo model and LCM are close to ideal. In addition, Newell model, Del Castillo model, and LCM necessitate only three parameters with Newell model featuring a particularly simple functional form.

ACKNOWLEDGEMENTS.

This research is partly sponsored by University Transportation Center (UTC) research grants. The authors thank the NGSIM program, FHWA, Georgia DOT, Caltrans, and all those who generously allowed access to their data sets which made this study possible. The authors would also like to thank Drs. Hesham Rakha, Martin Treiber, and Jose M. del Castillo for constructive discussions.

References

[1] R.E. Chandler, R. Herman, and E.W. Montroll. Traffic Dynamics: Studies in Car Following. *Operations Research*, 6:165–184, 1958.

[2] D. C. Gazis, R. Herman, and R. W. Rothery. Non-Linear Follow the Leader Models of Traffic Flow. *Operations Research*, 9:545–567, 1961.

[3] P.G. Gipps. A Behavioral Car Following Model for Computer Simulation. *Transportation Research, Part B*, 15:105–111, 1981.

[4] R. Wiedemann. *Simulation des Straenverkehrsflusses*. PhD thesis, Schriftenreihe des Instituts fr Verkehrswesen der Universitt Karlsruhe, Germany, 1974.

[5] S. Kikuchi and P. Chakroborty. Car-Following Model Based on a Fuzzy Inference System. *Transportation Research Record*, 1365:82–91, 1992.

[6] I. Kosonen. *HUTSIM - Urban Traffic Simulation and Control Model: Principles and Applications*. PhD thesis, Helsinki University of Technology, 1999.

[7] S. Panwai and H. F. Dia. A Reactive Agent-based Neural Network Car Following Model. In *8th International IEEE Conference on Interlligent Transportation Systems (ITSC2005)*, pages 326–331, Vienna, Austria, 2005.

[8] B.D. Greenshields. A study of Traffic Capacity. *Proceedings of Highway Research Board*, 14:448–477, 1934.

[9] A. D St. John. Grade Effects on Traffic Flow Stability And Capacity. Technical report, National Cooperative Highway Research Report 185. Transportation Research Board, National Research Council, 1978.

[10] FMCSA. FMCSA Part 571: Federal Motor Vehicle Safety Standards: Standard No. 105; Hydraulic and Electric Brake Systems 2005. http://www.fmcsa.dot.gov/, 1999.

[11] The Next Generation Simulation (NGSIM) Program. http://ngsim-community.org/, Accessed on March 12, 2011.

[12] S A Smith. Freeway Data Collection for Studying Vehicle Interactions - Technical Report. Final Report. Technical report, JHK & Associates and Federal Highway Administration, 1985.

[13] Integrated Vehicle-Based Safety Systems. http://www.its.dot.gov/ivbss/, Accessed on March 12, 2011.

[14] Martin Treiber, Ansgar Hennecke, , and Dirk Helbing. Congested Traffic States in Empirical Observations and Microscopic Simulations. *Phys. Rev. E*, 62:18051824, 2000.

[15] D. Helbing, A. Hennecke, V. Shvetsov, and M. Treiber. Micro- and Macro-Simulation of Freeway Traffic. *Mathematical and Computer Modelling*, 35(5):517–547, 2002.

[16] G. F. Newell. Nonlinear Effects in the Dynamics of Car Following. *Operations Research*, 9(2):209–229, 1961.

[17] M. Van Aerde. Single Regime Speed-Flow-Density Relationship for Congested and Uncongested Highways. In *Presented at the 74th Transportation Research Board (TRB) Annual Meeting, Paper number 950802*, Washington, D.C., 1995.

[18] M. Van Aerde and H. Rakha. Multivariate Calibration of Single Regime Speed-Flow-Density Relationships. In *Proceedings of the 6th 1995 Vehicle Navigation and Information Systems Conference*, pages 334–341, Seattle, WA, USA, 1995.

[19] J. M. Del Castillo and F. G. Bentez. On the Functional Form of the Speed-Density Relationship - I: General Theory. *Transportation Research Part B: Methodological*, 29(5):373–389, 1995.

[20] J. M. Del Castillo and F. G. Bentez. On the Functional Form of the Speed-Density Relationship - II: Empirical Investigation . *Transportation Research Part B: Methodological*, 29(5):391–406, 1995.

Received: November 25, 2012